Rotationally invariant *ab initio* evaluation of Coulomb and exchange parameters for DFT+U calculations

Nicholas J. Mosey,[1] Peilin Liao,[2] and Emily A. Carter[1,a]

[1]*Department of Mechanical and Aerospace Engineering and Program in Applied and Computational Mathematics, Princeton University, Princeton, New Jersey 08544-5263, USA*
[2]*Department of Chemistry, Princeton University, Princeton, New Jersey 08544-5263, USA*

Conventional density functional theory (DFT) fails for strongly correlated electron systems due to large intra-atomic self-interaction errors. The DFT+U method provides a means of overcoming these errors through the use of a parametrized potential that employs an exact treatment of quantum mechanical exchange interactions. The parameters that enter into this potential correspond to the spherically averaged intra-atomic Coulomb (U) and exchange (J) interactions. Recently, we developed an *ab initio* approach for evaluating these parameters on the basis of unrestricted Hartree–Fock (UHF) theory, which has the advantage of being free of self-interaction errors and does not require experimental input [Mosey and Carter, Phys. Rev. B **76**, 155123 (2007)]. In this work, we build on that method to develop a more robust and convenient *ab initio* approach for evaluating U and J. The new technique employs a relationship between U and J and the Coulomb and exchange integrals evaluated using the entire set of UHF molecular orbitals (MOs) for the system. Employing the entire set of UHF MOs renders the method rotationally invariant and eliminates the difficulty in selecting unambiguously the MOs that correspond to localized states. These aspects overcome two significant deficiencies of our earlier method. The new technique is used to evaluate U and J for Cr_2O_3, FeO, and Fe_2O_3. The resulting values of U-J are close to empirical estimates of this quantity for each of these materials and are also similar to results of constrained DFT calculations. DFT+U calculations using the *ab initio* parameters yield results that are in good agreement with experiment. As such, this method offers a means of performing accurate and fully predictive DFT+U calculations of strongly correlated electron materials. © *2008 American Institute of Physics*. [DOI: 10.1063/1.2943142]

I. INTRODUCTION

The Kohn–Sham density functional theory [1–5] (DFT) has become the method of choice for performing electronic structure calculations of materials and molecules represented by models containing up to a few hundred atoms. These calculations have shed light on a wide range of phenomena that would be difficult, or impossible, to study experimentally with atomic-level resolution. Despite the clear capabilities of DFT, phenomena and systems exist for which the method fails not just quantitatively but even qualitatively. These deficiencies arise primarily from the use of approximate exchange-correlation (XC) functionals. Overcoming these limitations awaits the development of new XC functionals and alternative computationally efficient methods that incorporate the essential physics missing in existing functionals.

Strongly correlated electron materials (SCEMs) are an important class of systems that are not described accurately by DFT. Typical SCEMs have partially filled, tightly contracted d and f orbitals, such as in mid-to-late first row transition metal oxides and actinides. The Coulomb repulsion between these d or f electrons is intrinsically large due to the

contracted nature of the multiply charged transition metal ion or actinide metal orbitals, leading to a high degree of correlation between their motions and to narrow widths for the bands associated with these electrons. If the localized electronic states are close to the Fermi level, the material becomes an insulator. DFT calculations tend to characterize SCEMs as metals or small-gap insulators. This failure of DFT is a result of using approximate XC functionals. Specifically, the intra-atomic Coulomb and exchange energies associated with the localized states are large because of the significant number of open-shell electrons and the particularly tight nature of the wavefunctions involved. Due to the approximate treatment of exchange, XC functionals fail to cancel exactly the self-interaction energy, which manifests as a spurious electron-electron repulsion. To minimize this repulsion, DFT calculations delocalize these electronic states, leading to a reduction in the band gap. Although this self-interaction error is present in any material with open-shell electrons, the error is particularly egregious for SCEMs due to the particularly large intra-atomic exchange energies, each of which is poorly accounted for.

Obtaining an accurate description of the electronic structure of SCEMs thus rests on the ability to properly remove the self-interaction energies of the localized electrons. A natural approach to eliminating self-interaction is through the

a)Author to whom correspondence should be addressed. Electronic mail: eac@princeton.edu.

use of the Hartree–Fock (HF) theory which includes exact exchange. Unfortunately, the neglect of static and dynamic correlation effects in HF limits its accuracy, particularly in overestimating Coulomb repulsion, leading to band gaps that are far too large. Post-HF *ab initio* methods that capture at least some of the correlation effects are quite expensive computationally, and, for the most part, have not been implemented for periodic systems.[6–9] Hybrid DFT functionals that incorporate a degree of HF exchange also offer a possible means of treating SCEMs. However, this approach applies partial HF exchange equally to all electrons in the material. It is well known that HF band energies exhibit an unphysical logarithmic singularity at the Fermi level, which produces spurious charge and spin density waves in metals. This suggests that any delocalized electrons in SCEMs that are akin to electrons in metals will not be treated properly by hybrid DFT. Although evaluating HF exchange with the plane-wave basis sets typically used to study periodic systems is computationally expensive, hybrid functionals have been incorporated into such codes recently and have been applied to SCEMs.[10–12]

In the absence of a single method that captures electron correlation and eliminates self-interaction while remaining computationally efficient, the development of methods for performing electronic structure calculations of SCEMs has focused on combining different methods that meet at least one of these criteria. In general, these approaches divide the electronic structure into localized and delocalized states, and apply appropriate methodologies to each subsystem. The most commonly used method based on this approach is called DFT+U.[13,14] The DFT+U technique uses a HF-like potential to describe the interactions between electrons localized on the same atomic center (called on-site interactions) and uses DFT to describe all other interactions in the system. This combination makes physical sense because use of HF for the intra-atomic exchange interactions between the localized open-shell electrons eliminates self-interaction error while the use of DFT provides the best description available of the delocalized electrons.

In practice, the on-site energy in a DFT+U calculation is evaluated with a parameterized HF-like potential. This has the benefit of avoiding an explicit HF calculation, facilitating the incorporation of the DFT+U method into existing periodic DFT codes employing plane-wave basis sets, while engendering little computational overhead compared to a standard DFT calculation. The parameters that enter into the HF-like potential correspond to spherically averaged Coulomb and exchange interactions between electrons of a particular angular momentum that are localized on the same atom. These parameters are called $U_{I\ell}$ (Coulomb) and $J_{I\ell}$ (exchange), where I denotes the atomic center on which the electrons are localized and ℓ denotes their angular momentum. In order to perform accurate DFT+U calculations, one must provide values of these parameters that reasonably reflect the strengths of the on-site interactions in the material of interest. Conventionally, this has been done in either of two ways. In one case, the parameters are treated as empirical values and are adjusted to best reproduce experimental data when used in DFT+U calculations.[15,16] This approach

requires experimental data, which prevents its application in a predictive sense. Moreover, no underlying physical basis exists for selecting a particular set of empirical values. The second typical approach involves constrained DFT calculations, which evaluate $U_{I\ell}$ and $J_{I\ell}$ using relationships between the energy of the system and the number of localized electrons.[17–19] This method suffers from the same deficiencies of DFT that necessitated the development of the DFT+U methodology, and yields parameters that depend on the XC functional, which is inconsistent with the fact that from a physical standpoint, the on-site interaction energies should be constant for a given material.

Recently, we developed an *ab initio* approach for evaluating $U_{I\ell}$ and $J_{I\ell}$ that was based on HF calculations of electrostatically embedded atomic clusters representing the bulk material of interest.[20] This method employed a mapping between $U_{I\ell}$ and $J_{I\ell}$ and the Coulomb and exchange integrals evaluated in the subset of unrestricted HF (UHF) molecular orbitals (MOs) corresponding to the localized states in the system. The scheme does not rely on any experimental input, and hence can be used to evaluate $U_{I\ell}$ and $J_{I\ell}$ for DFT+U calculations of novel systems. In addition, the calculated values of $U_{I\ell}$ and $J_{I\ell}$ have the advantage of being derived from an *ab initio* theory that is free of self-interaction errors. The technique was used to evaluate $U_{I\ell}$ and $J_{I\ell}$ for the 3d electrons localized on the Cr atoms of Cr_2O_3, and the resulting values for these parameters yielded satisfactory results when used in DFT+U calculations. However, more recent application of this method to other systems and scenarios, e.g., FeO and Cr_2O_3 surfaces, exposed some of its deficiencies. These include difficulties in unambiguously selecting the UHF MOs corresponding to the localized states, the lack of invariance with respect to unitary transformations of the entire set of UHF MOs, and the tendency to provide values of $U_{I\ell}$ and $J_{I\ell}$ that are somewhat too large to be of general use in DFT+U calculations.

In the present work, we introduce and test a new *ab initio* approach for calculating $U_{I\ell}$ and $J_{I\ell}$ that overcomes the deficiencies associated with our previous method. The new scheme is also based on UHF calculations of electrostatically embedded clusters representing the material of interest, but the definitions of $U_{I\ell}$ and $J_{I\ell}$ are based on the Coulomb and exchange integrals evaluated using all of the UHF MOs. Employing the entire set of UHF MOs overcomes the need to select a subset of MOs as the localized states and retains rotational invariance. Tests demonstrate that this method consistently yields values of $U_{I\ell}$ and $J_{I\ell}$ that are suitable for DFT+U calculations.

The capabilities of the new method will be demonstrated by evaluating $U_{I\ell}$ and $J_{I\ell}$ for Cr_2O_3, FeO, and Fe_2O_3. In each case, the calculated values of $U_{I\ell}$-$J_{I\ell}$ are in good agreement with previously reported values obtained through either empirical means or constrained DFT calculations. The results demonstrate that the new method (i) yields values of $U_{I\ell}$-$J_{I\ell}$ that are in better agreement with empirical estimates of these quantities than those obtained with our earlier approach, (ii) exhibits the correct sensitivity to the electronic state of the system (the strengths of the on-site interactions for a given material are lower when the material is in a ferromagnetic

state than when it is in an antiferromagnetic state), and (iii) exhibits the correct sensitivity to the oxidation state of the transition metal ion (the strengths of the on-site interactions for the Fe^{3+} ions in Fe_2O_3 are larger than those of the Fe^{2+} ions in FeO). Subsequent DFT+U calculations show that the *ab initio* parameters yield results that are in satisfactory agreement with experimental data.

The work is presented as follows. In the next section, DFT+U theory is discussed briefly and the *ab initio* method for evaluating $U_{I\ell}$ and $J_{I\ell}$ is outlined. In Sec. III, this technique is used to evaluate $U_{I\ell}$ and $J_{I\ell}$ for Cr_2O_3, FeO, and Fe_2O_3. In Sec. IV, DFT+U calculations of bulk Cr_2O_3, FeO, and Fe_2O_3 are used to determine how well the *ab initio* parameters reproduce experimental results. The conclusions are provided in Sec. V.

II. METHODOLOGY

The goal of this work is to develop and test an *ab initio* method for evaluating the parameters $U_{I\ell}$ and $J_{I\ell}$ that enter into DFT+U calculations. The development of the new methodology is outlined in this section. Section II A provides a brief overview of the DFT+U method. The new *ab initio* technique is outlined in Sec. II B, and its implementation into the GAMESS electronic structure package[21,22] is discussed in Sec. II C.

A. DFT+U

The DFT+U method[13,14] employs a HF treatment of the on-site interactions, which are characterized as interactions between electrons of the same angular momentum ℓ that are localized in atomic-like orbitals on the same atom I, and uses DFT methods to describe all other interactions in the system. This is achieved with the following general functional form:

$$E^{\mathrm{DFT+U}}[\rho,\{n_{I\ell m\sigma}\}]$$
$$= E^{\mathrm{DFT}}[\rho] + E^{\mathrm{on\text{-}site}}[\{n_{I\ell m\sigma}\}] - E^{\mathrm{dc}}[\{N_{I\ell\sigma}\}], \quad (1)$$

where E^{DFT} is the DFT energy of the system based on the total electron density ρ, $E^{\mathrm{on\text{-}site}}$ is the on-site energy, and E^{dc} is a double-counting term that corrects for the fact that the on-site interactions are included in both E^{DFT} and $E^{\mathrm{on\text{-}site}}$. $n_{I\ell m\sigma}$ corresponds to the number of electrons with spin σ, angular momentum ℓ, and magnetic quantum number m that are localized on atom I. In practice, the values of $n_{I\ell m\sigma}$ are obtained by projecting the Kohn–Sham orbitals for the entire system onto a suitable set of atom-centered basis functions. The quantity $N_{I\ell\sigma}$ is the number of electrons of angular momentum ℓ and spin σ that are localized on atom I and is given by $N_{I\ell\sigma}=\Sigma_m n_{I\ell m\sigma}$.

Here, we will focus on the DFT+U formalism developed by Dudarev *et al.*,[23] which is implemented in the VASP electronic structure package.[24,25] In this formalism, $E^{\mathrm{on\text{-}site}}$ and E^{dc} are defined as

$$E^{\mathrm{on\text{-}site}}[\{n_{I\ell m\sigma}\}] = \left(\sum_{m,m'} n_{I\ell m\alpha}n_{I\ell m'\beta} + \sum_{m,m'>m} n_{I\ell m\alpha}n_{I\ell m'\alpha} \right.$$
$$\left. + \sum_{m,m'>m} n_{I\ell m\beta}n_{I\ell m'\beta} \right) U_{I\ell}$$
$$- \left(\sum_{m,m'>m} n_{I\ell m\alpha}n_{I\ell m'\alpha} \right.$$
$$\left. + \sum_{m,m'>m} n_{I\ell m\beta}n_{I\ell m'\beta} \right) J_{I\ell}, \quad (2)$$

$$E^{\mathrm{dc}}[\{N_{I\ell\sigma}\}] = \left(N_{I\ell\alpha}N_{I\ell\beta} + \frac{N_{I\ell\alpha}(N_{I\ell\alpha}-1)}{2} \right.$$
$$\left. + \frac{N_{I\ell\beta}(N_{I\ell\beta}-1)}{2} \right) U_{I\ell} - \left(\frac{N_{I\ell\alpha}(N_{I\ell\alpha}-1)}{2} \right.$$
$$\left. + \frac{N_{I\ell\beta}(N_{I\ell\beta}-1)}{2} \right) J_{I\ell}. \quad (3)$$

Note that for the sake of clarity these definitions have been written to describe the on-site and double-counting energies arising from electrons of a particular angular momentum on a single atom. In a polyatomic system, there would be a summation over multiple atoms and different values of ℓ in accordance with the nature of the localized electrons in the system.

The quantities $U_{I\ell}$ and $J_{I\ell}$ in Eqs. (2) and (3) correspond to the spherically averaged Coulomb and exchange interactions between electrons of angular momentum ℓ that are localized on the same atom I. Using these quantities, Eq. (2) provides a HF-like treatment of the on-site interaction energies, assuming that the Coulomb and exchange interactions are independent of m. The expression for E^{dc} is approximate and essentially enumerates the on-site interactions that are accounted for in E^{DFT}. Justifications for this particular form of E^{dc} have been made elsewhere,[23] and will not be discussed here.

Inserting the definitions of $E^{\mathrm{on\text{-}site}}$ and E^{dc} in Eqs. (2) and (3) into Eq. (1) leads to the following expression for $E^{\mathrm{DFT+U}}$:

$$E^{\mathrm{DFT+U}}[\rho,\{n_{I\ell m\sigma}\}]$$
$$= E^{\mathrm{DFT}}[\rho] + \sum_{I,\ell,m,\sigma} \frac{(U_{I\ell}-J_{I\ell})}{2}(n_{I\ell m\sigma} - n_{I\ell m\sigma}^2), \quad (4)$$

where the summation in the second term on the right-hand side has been written in a general sense for a polyatomic system. In practice, this summation would only include values of I and ℓ that are consistent with the localized electrons of the system. Unfortunately, this expression is not invariant with respect to unitary transformations of orbitals. To achieve rotational invariance, the occupation numbers in Eq. (4) must be replaced by the on-site density matrix of the localized electrons $\rho_{jk}^{I\ell\sigma}$.[23] Doing this leads to the following DFT+U total energy functional:

$$E^{\text{DFT+U}}[\rho] = E^{\text{DFT}}[\rho] + \sum_{I,\ell,\sigma} \frac{(U_{I\ell} - J_{I\ell})}{2}$$

$$\times \left[\sum_j \rho_{jj}^{I\ell\sigma} - \sum_{j,k} \rho_{jk}^{I\ell\sigma} \rho_{kj}^{I\ell\sigma} \right]. \quad (5)$$

Note that Eqs. (4) and (5) are equivalent when the on-site density matrix is diagonal.

The first term on the right-hand side of Eq. (5) corresponds to the DFT energy based on the total electron density of the system and the second term can be interpreted as a penalty function that modulates the electron density associated with the localized states. Noting that $U_{I\ell} > J_{I\ell}$ and $\sum_{jk}[\rho_{jj}^{I\ell\sigma} - \rho_{jk}^{I\ell\sigma}\rho_{kj}^{I\ell\sigma}] > 0$, it becomes evident that this is a positive definite penalty function driving the on-site density matrix toward idempotency. This property of the penalty function biases the localized states toward integer occupations, which counters the tendency of DFT calculations to fractionally occupy these states (as in a metal).

The one-electron potential $V_{jk}^{I\ell\sigma}$ of the localized orbitals can be obtained by differentiating $E^{\text{DFT+U}}$ with respect to $\rho_{jk}^{I\ell\sigma}$,

$$V_{jk}^{I\ell\sigma} = \frac{\delta E^{\text{DFT}}}{\delta \rho_{jk}^{I\ell\sigma}} + (U_{I\ell} - J_{I\ell})\left(\frac{1}{2}\delta_{jk} - \rho_{kj}^{I\ell\sigma} \right). \quad (6)$$

In the limit of integer occupations of the localized states, this has the effect of shifting the energies of the occupied localized orbitals by $-(U_{I\ell}-J_{I\ell})/2$ and the energies of the unoccupied localized orbitals by $(U_{I\ell}-J_{I\ell})/2$, increasing the band gap by $U_{I\ell}-J_{I\ell}$. This property counteracts the tendency of DFT calculations to greatly underestimate the band gaps of SCEMs.

B. *Ab initio* method for calculating *U* and *J*

Obtaining reasonable results from DFT+U calculations is entirely dependent on selecting appropriate values of $U_{I\ell}$ and $J_{I\ell}$. As noted above, conventional approaches for selecting these parameters involve either empirical fitting or constrained DFT calculations—both of which suffer from deficiencies. Previously, we developed an *ab initio* approach for evaluating $U_{I\ell}$ and $J_{I\ell}$ that was based on the notion that the on-site energy is a material-dependent quantity that can be approximated with HF calculations.[20] That approach involved a mapping between $E^{\text{on-site}}$ in Eq. (2) and the Coulomb and exchange integrals evaluated using the subset of UHF MOs corresponding to the localized states in the system. As noted above, that method has some deficiencies, including a lack of invariance with respect to unitary transformations of the entire set of UHF MOs and difficulties in unambiguously specifying the UHF MOs that correspond to the localized states. In what follows, we will develop a new *ab initio* approach for evaluating $U_{I\ell}$ and $J_{I\ell}$ that employs the entire set of occupied UHF MOs. This will preserve rotational invariance and eliminate the complications associated with selecting a subset of the MOs corresponding to the localized states.

The first step in evaluating $U_{I\ell}$ and $J_{I\ell}$ through UHF calculations is to express the on-site interaction energy in terms of Coulomb and exchange integrals evaluated in the basis of the UHF MOs. These integrals are expressed as

$$C_{ij}^{\sigma\sigma'} = N_{i\sigma}N_{j\sigma'} \int \int \frac{\phi_{i\sigma}(\mathbf{r}_1)\phi_{i\sigma}(\mathbf{r}_1)\phi_{j\sigma'}(\mathbf{r}_2)\phi_{j\sigma'}(\mathbf{r}_2)}{|\mathbf{r}_1 - \mathbf{r}_2|} d\mathbf{r}_1 d\mathbf{r}_2, \quad (7)$$

and

$$X_{ij}^{\sigma\sigma} = N_{i\sigma}N_{j\sigma} \int \int \frac{\phi_{i\sigma}(\mathbf{r}_1)\phi_{i\sigma}(\mathbf{r}_2)\phi_{j\sigma}(\mathbf{r}_1)\phi_{j\sigma}(\mathbf{r}_2)}{|\mathbf{r}_1 - \mathbf{r}_2|} d\mathbf{r}_1 d\mathbf{r}_2, \quad (8)$$

where $C_{ij}^{\sigma\sigma'}$ is a Coulomb integral, $X_{ij}^{\sigma\sigma}$ is an exchange integral, and $\phi_{i\sigma}$ is a UHF MO. $N_{i\sigma}$ is the occupation number of $\phi_{i\sigma}$, which is equal to 1 for occupied UHF MOs. Note that an unconventional nomenclature has been employed to avoid confusion with other quantities considered in this work (typically Coulomb integrals would be labeled U or J, and exchange integrals would be designated as J or K). In principle, $N_{i\sigma}$ can be decomposed into contributions from electrons located in atomic orbitals (AOs) throughout the system

$$N_{i\sigma} = \sum_{I,\ell} n_{i\sigma I\ell} = 1 \quad (9)$$

where $n_{i\sigma I\ell}$ is the number of electrons in an AO of angular momentum ℓ localized on atom I that contribute to the total population of MO $\phi_{i\sigma}$. $n_{i\sigma I\ell}$ can be obtained by projecting the total wavefunction onto a set of atom-centered basis functions with well-defined angular momenta. Details regarding the evaluation of these populations are discussed in Sec. III C.

Inserting Eq. (9) into Eqs. (7) and (8), keeping all the terms where I and ℓ are the same and have values associated with localized states, and summing over all allowed pairs of MOs leads to the following expression for the on-site interaction energy evaluated in the basis of the occupied UHF MOs:

$$E_{\text{HF}}^{\text{on-site}} = \sum_{i,j} n_{i\alpha I\ell}n_{j\beta I\ell}C_{ij}^{\alpha\beta} + \sum_{i,j>i} n_{i\alpha I\ell}n_{j\alpha I\ell}C_{ij}^{\alpha\alpha}$$

$$+ \sum_{i,j>i} n_{i\beta I\ell}n_{j\beta I\ell}C_{ij}^{\beta\beta} - \sum_{i,j>i} n_{i\alpha I\ell}n_{j\alpha I\ell}X_{ij}^{\alpha\alpha}$$

$$- \sum_{i,j>i} n_{i\beta I\ell}n_{j\beta I\ell}X_{ij}^{\beta\beta}. \quad (10)$$

$E_{\text{HF}}^{\text{on-site}}$ provides an estimate of the true on-site interaction energy in the material, and should equal the quantity given by Eq. (2). Setting Eq. (10) equal to Eq. (2), and treating the Coulomb and exchange terms separately leads to the following expressions for $U_{I\ell}$ and $J_{I\ell}$:

$$U_{I\ell} = \frac{\sum_{i,j} n_{i\alpha I\ell} n_{j\beta I\ell} C_{ij}^{\alpha\beta} + \sum_{i,j>i} n_{i\alpha I\ell} n_{j\alpha I\ell} C_{ij}^{\alpha\alpha} + \sum_{i,j>i} n_{i\beta I\ell} n_{j\beta I\ell} C_{ij}^{\beta\beta}}{\sum_{m,m'} n_{I\ell m\alpha} n_{I\ell m'\beta} + \sum_{m,m'>m} n_{I\ell m\alpha} n_{I\ell m'\alpha} + \sum_{m,m'>m} n_{I\ell m\beta} n_{I\ell m'\beta}}, \tag{11}$$

and

$$J_{I\ell} = \frac{\sum_{i,j>i} n_{i\alpha I\ell} n_{j\alpha I\ell} X_{ij}^{\alpha\alpha} + \sum_{i,j>i} n_{i\beta I\ell} n_{j\beta I\ell} X_{ij}^{\beta\beta}}{\sum_{m,m'>m} n_{I\ell m\alpha} n_{I\ell m'\alpha} + \sum_{m,m'>m} n_{I\ell m\beta} n_{I\ell m'\beta}}, \tag{12}$$

where the numerator in each expression is the total Coulomb or exchange energy arising from interactions between electrons of angular momentum ℓ that are localized on atom I evaluated in the basis of the UHF MOs. The denominator in each case enumerates the number of on-site Coulomb and exchange interactions weighted by the number of electrons involved in those interactions. In this sense, these equations provide the average on-site Coulomb and exchange interactions, which are precisely the quantities represented by the parameters $U_{I\ell}$ and $J_{I\ell}$. Up to this point, the expressions derived for $U_{I\ell}$ and $J_{I\ell}$ above are identical to our earlier proposal.[20] The difference lies in the limits on the summations: Our earlier work summed only over selected localized orbitals whereas the current formalism sums over all occupied MOs.

C. Implementation

The ability to evaluate $U_{I\ell}$ and $J_{I\ell}$ according to Eqs. (11) and (12) has been implemented into the GAMESS electronic structure package.[21,22] Those equations represent the on-site interactions in terms of the Coulomb and exchange integrals evaluated in the basis of the entire set of occupied UHF MOs. In practice, it is computationally intensive to evaluate these integrals. However, the use of the entire set of MOs permits the evaluation of Eqs. (11) and (12) through a procedure analogous to the construction of density and Fock matrices used in standard UHF calculations, thereby avoiding the explicit evaluation of the Coulomb and exchange integrals in the molecular orbital basis. The details of this implementation are discussed in what follows.

The starting point for evaluating $U_{I\ell}$ and $J_{I\ell}$ involves the calculation of $n_{i\sigma I\ell m}$, which corresponds to the number of electrons in each atomic-like orbital of angular momentum ℓ and magnetic quantum number m localized on atom I that contributes to the total population of molecular orbital $\phi_{i\sigma}$. The values of $n_{i\sigma I\ell m}$ will be used to construct $n_{i\sigma I\ell}$ and $n_{I\ell m\sigma}$. Noting that in GAMESS and many other electronic structure codes the MOs $\phi_{i\sigma}$ are expressed as a linear combination of atom-centered basis functions χ_μ that have well-defined values of ℓ and m, i.e., $\phi_i = \sum_\mu c_{i\mu} \chi_\mu$, the Mulliken population analysis is used to equate $n_{i\sigma I\ell m}$ with the contribution of all basis functions with the quantum numbers ℓ and m centered on atom I to the total population of molecular orbital $\phi_{i\sigma}$,

$$n_{i\sigma I\ell m} = \sum_\mu n_{i\sigma\mu} = \sum_\mu \sum_\nu c_{i\mu} c_{i\nu} \langle \mu | \nu \rangle, \tag{13}$$

where μ runs over all basis functions with the appropriate values of I, ℓ, and m, ν runs over all basis functions, and $\langle \mu | \nu \rangle$ is the overlap integral between basis functions χ_μ and χ_ν. The summation over μ accounts for the fact that in many common basis sets there is more than one basis function associated with each value of m. Altogether, there will be $2\ell+1$ values of $n_{i\sigma I\ell m}$ for each ℓ on a particular atom.

Equation (13) provides the basic quantities needed to construct the populations $n_{i\sigma I\ell}$ and $n_{I\ell m\sigma}$. The former represents the total number of electrons of angular momentum ℓ localized on atom I that are present in MO $\phi_{i\sigma}$, and is expressed as $n_{i\sigma I\ell} = \sum_m n_{i\sigma I\ell m}$. The latter represents the total number of electrons in the system associated with a specific set of I, ℓ, m, and σ, and is expressed as $n_{I\ell m\sigma} = \sum_i n_{i\sigma I\ell m}$, where the index i runs over all occupied MOs.

The values of $n_{i\sigma I\ell}$ can be used in conjunction with the MO coefficients to construct a density matrix,

$$P_{\mu\nu}^\sigma = \sum_i n_{i\sigma I\ell} c_{i\mu}^\sigma c_{i\nu}^\sigma, \tag{14}$$

which can be used to construct the Coulomb ($C_{\mu\nu}^\sigma$) and exchange ($X_{\mu\nu}^\sigma$) matrix elements,

$$C_{\mu\nu}^\sigma = \sum_\kappa \sum_\lambda P_{\kappa\lambda}^\sigma (\mu\nu|\kappa\lambda) + \sum_\kappa \sum_\lambda P_{\kappa\lambda}^{-\sigma} (\mu\nu|\kappa\lambda), \tag{15}$$

and

$$X_{\mu\nu}^\sigma = \sum_\kappa \sum_\lambda P_{\kappa\lambda}^\sigma (\mu\lambda|\kappa\nu), \tag{16}$$

where $(\mu\nu|\kappa\lambda)$ is a two-electron integral evaluated in the atomic orbital basis. Note that $C_{\mu\nu}^\sigma$ and $X_{\mu\nu}^\sigma$ are not equal to the Coulomb and exchange integrals written in Eqs. (7) and (8), but instead are contributions to the Fock matrix that can be evaluated independently to calculate the total Coulomb and exchange energies. The total Coulomb and exchange energies, designated C and X, respectively, can be obtained by multiplying the Coulomb and exchange matrices by the density matrix

$$C = 0.5 \left(\sum_{\mu\nu} P_{\mu\nu}^\alpha C_{\nu\mu}^\alpha + \sum_{\mu\nu} P_{\mu\nu}^\beta C_{\nu\mu}^\beta \right), \tag{17}$$

and

$$X = 0.5 \left(\sum_{\mu\nu} P_{\mu\nu}^\alpha X_{\nu\mu}^\alpha + \sum_{\mu\nu} P_{\mu\nu}^\beta X_{\nu\mu}^\beta \right). \tag{18}$$

Equations (17) and (18) provide the on-site Coulomb and exchange interaction energies evaluated in the atomic orbital basis, which is much more efficient computationally than performing the transformation needed to evaluate these quantities in the MO basis. Unfortunately, these energies

contain self-interaction errors, which must be removed before one can calculate $U_{I\ell}$ and $J_{I\ell}$. The self-interaction energy contained in Eqs. (17) and (18) is evaluated as

$$\text{SI} = 0.5\left(\sum_i n_{i\alpha I\ell}n_{i\alpha I\ell}C_{ii}^{\alpha\alpha} + \sum_i n_{i\beta I\ell}n_{i\beta I\ell}C_{ii}^{\beta\beta}\right), \quad (19)$$

where the index i runs over all occupied molecular orbitals of α or β spin and $C_{ii}^{\sigma\sigma}$ represents the Coulomb integral involving an electron in orbital $\phi_{i\sigma}$ interacting with itself. These integrals must be evaluated in the MO basis, which is computationally expensive and forms the computational bottleneck in the evaluation of $U_{I\ell}$ and $J_{I\ell}$. To improve efficiency, we have implemented a population cutoff in which

the self-interaction integrals are evaluated only if the occupation number $n_{i\sigma I\ell}$ associated with the MO is above a certain threshold. Otherwise, the integral is set to zero. Experience shows that neglecting all integrals with values of $n_{i\sigma I\ell}$ less than 5.0×10^{-3} reduces significantly the number of self-interaction integrals that must be calculated, yet only affects the values of $U_{I\ell}$ and $J_{I\ell}$ on the order of 0.01 eV, which is too small an error to affect the results of subsequent DFT +U calculations.

Using Eqs. (17)–(19) along with the definition of $n_{I\ell m\sigma}$ provided above leads to the following expressions for $U_{I\ell}$ and $J_{I\ell}$:

$$U_{I\ell} = \frac{C - \text{SI}}{\Sigma_{m,m'}n_{I\ell m\alpha}m_{I\ell m'\beta} + \Sigma_{m,m'>m}n_{I\ell m\alpha}n_{I\ell m'\alpha} + \Sigma_{m,m'>m}n_{I\ell m\beta}n_{I\ell m'\beta}}, \quad (20)$$

and

$$J_{I\ell} = \frac{X - \text{SI}}{\Sigma_{m,m'>m}n_{I\ell m\alpha}n_{I\ell m'\alpha} + \Sigma_{m,m'>m}n_{I\ell m\beta}n_{I\ell m'\beta}}. \quad (21)$$

These expressions are equivalent to those in Eqs. (11) and (12), but minimize the number of terms evaluated in the MO basis, leading to a significant improvement in efficiency. In this implementation, evaluating the occupation numbers through the Mulliken population analysis incurs a minimal cost, calculating C and X incurs a cost that is approximately equivalent to that of two SCF iterations, and the cost of evaluating the self-interaction integrals without a population cutoff scales linearly with the number of occupied MOs. As noted above, the calculation of the self-interaction energy is the computational bottleneck, and can be reduced significantly by using a population cutoff to avoid calculating self-interaction integrals for MOs with small populations of localized electrons.

III. EVALUATION OF *U* AND *J* FOR Cr_2O_3, FeO, AND Fe_2O_3

The method described in Sec. II was used to evaluate the parameters $U_{I\ell}$ and $J_{I\ell}$ for Cr_2O_3 (chromia), FeO (wüstite), and Fe_2O_3 (hematite). Since the only localized electrons in each of these systems correspond to $3d$ electrons localized on the transition metal atoms, we will simply refer to $U_{I\ell}$ and $J_{I\ell}$ as U and J, respectively. The rationale for exploring these particular systems is as follows. Cr_2O_3 was the focus of an earlier study in which we presented another *ab initio* approach for determining U and J.[20] Since the method reported in Sec. II aims to improve on the deficiencies of our earlier approach, studying this material again will allow us to examine how the values of U and J obtained with the current method differ from those reported previously. FeO is a material whose electronic structure does not permit the unambiguous identification of canonical HF MOs of a highly lo-

calized nature, which is necessary for evaluating U and J with our earlier method. As such, evaluating U and J for this system will demonstrate how the new approach overcomes practical limitations of our earlier method. The iron atoms in Fe_2O_3 are in a different oxidation state (Fe^{3+}) than those in FeO (Fe^{2+}). The d orbitals on Fe^{3+} ions are expected to be more contracted than those on Fe^{2+} ions and, consequently, the values of U and J are expected to be higher in Fe_2O_3 than in FeO. Thus, by evaluating U and J for Fe_2O_3 and comparing the results with those obtained for FeO, we will be able to assess the sensitivity of the approach described in Sec. II to the oxidation state of the transition metal. We further note that our motivation for developing an approach for calculating U and J stems from a related study exploring the mechanical properties of chromium-based coatings for steel surfaces. The fact that Cr_2O_3, FeO, and Fe_2O_3 are key materials in that system has also played a role in our selection of materials for the current study. The details of the UHF calculations performed to evaluate U and J are provided in Sec. III A and the results of the calculations are given in Sec. III B.

A. Calculation details

The values of U and J were evaluated for Cr_2O_3, FeO, and Fe_2O_3 by performing UHF calculations with a version of the GAMESS electronic structure package[21,22] that was modified as outlined in Sec. II. The calculations were performed using electrostatically embedded M_xO_y clusters, where M represents a transition metal atom. The clusters were based on the bulk structures of each material and were constructed by starting with a central M ion and adding successive shells of symmetrically equivalent M ions around the central ion along with enough O ions to ensure that each M was hexacoordinate as in the bulk. The clusters for the Cr_2O_3, FeO, and Fe_2O_3 systems ranged in size from CrO_6^{9-} to $Cr_{36}O_{96}^{84-}$, FeO_6^{10-} to $Fe_{43}O_{92}^{98-}$, and FeO_6^{9-} to $Fe_{36}O_{99}^{90-}$, respec-

tively. The charges were assigned assuming that the oxygen atoms have a net charge of $-2e$ in all materials, the Cr ions in Cr_2O_3 and the Fe ions in Fe_2O_3 have net charges of $+3e$, and the Fe ions in FeO have net charges of $+2e$. To incorporate bulk electrostatic effects, the clusters were embedded in an array of point charges with positions corresponding to those of the transition metal and oxygen atoms in the respective bulk materials. The point charges at the positions of transition metal atoms coordinated directly to the outermost oxygen atoms of the embedded cluster were replaced by Al effective core potentials[26] (ECPs) in the cases of Cr_2O_3 and Fe_2O_3 and Mg ECPs[26] in the case of FeO. The Al ECPs have a charge of $+3e$, equivalent to the formal charges of Cr and Fe in Cr_2O_3 and Fe_2O_3, and the Mg ECPs have a charge of $+2e$, equivalent to the formal charge of Fe in FeO. Tests showed that the calculated values of U-J were insensitive to the ECP used as long as the ionic radius of the atom represented by the ECP was similar to that of the ionic radius of the atom it was replacing in the point charge array. The Mg and Al ECPs were used because the ionic radius of Al^{3+} (67.5 pm) is similar to those of Cr^{3+} (75.5 pm) and Fe^{3+} (69.0 pm); the ionic radius of Mg^{2+} (86.0 pm) is similar to that Fe^{2+} (75.0 pm).[27] The ECPs provide a degree of exchange repulsion that prevents the artificial drift of electron density from the embedded cluster into the surrounding point charge array. The charges on the edges and faces of the point charge array were assigned fractional values according the method of Evjen.[28] All other point charges corresponding to oxygen atoms were assigned values of $-2e$, while those corresponding to the positions of transition metal atoms were assigned values of $+3e$ (Cr_2O_3 and Fe_2O_3) or $+2e$ (FeO). In all cases, the size of the point charge array was selected to ensure that the calculated values of U-J were converged to better than 0.1 eV.

Preliminary tests on small clusters demonstrated that the values of U-J were relatively insensitive to the basis set used on oxygen, varying by no more that 0.1 eV for the series of 6-31G(d), 6-311G(d), 6-31+G(d), cc-pvDZ, and DZP basis sets.[29–31] As such, all UHF calculations were performed using the 6-31G(d) basis set on oxygen. To explore the influence of the basis set on the transition metal atom, calculations were performed using the LANL2DZ (Ref. [26]) and the Stuttgart[32] basis sets on that atom. Both of these basis sets treat explicitly the $3s$, $3p$, $3d$, and $4s$ electrons of the transition metal, while representing all other electrons with an ECP. In the LANL2DZ basis set, the $3d$ electrons are treated with two sets of basis functions, and both sets of d-type basis functions were used in the Mulliken populations used to evaluate the orbital populations with Eq. (13). In the Stutgart basis set, these electronic states are treated with three sets of basis functions and only the tightest two sets of d-type basis functions were used to evaluate these populations. The most diffuse set of d-type basis functions included in the Stuttgart basis set was not used to evaluate the populations because they do not represent localized d orbitals, and including them in the calculation led to unphysical populations. In all cases, the angular components of the basis functions were represented by spherical harmonics, which simplified the population analysis. A set of calculations was
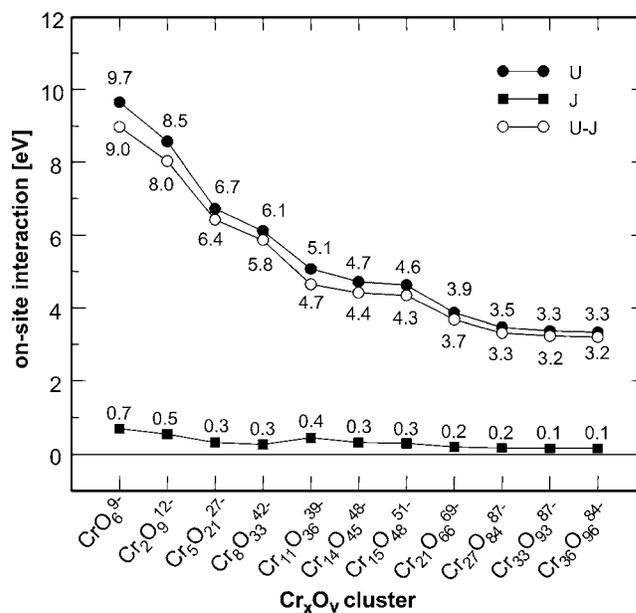

FIG. 1. U, J, and U-J for Cr_2O_3 as a function of cluster size. The clusters exhibited AFM spin ordering. All calculations were performed using the Stuttgart basis set on chromium and a 6-31G(d) basis set on oxygen. Converged values of U, J, and U-J are 3.3, 0.1, and 3.2 eV, respectively.

performed using clusters that exhibited the correct antiferromagnetic (AFM) ordering of the bulk materials. For Cr_2O_3, this corresponds to the sign of the net spin on the Cr ions alternating along the [0001] direction;[33–35] for Fe_2O_3, the sign of the net spin on the Fe ions exhibits a $++--$ pattern along the [0001] direction;[36] and for FeO, the sign of the net spin on the Fe ions alternates between neighboring (111) planes of Fe ions.[37] In addition, calculations were performed with each material exhibiting a ferromagnetic (FM) electronic structure to assess the sensitivity of the values of U, J, and U-J to the arrangement of the net spins in the material.

B. Results

Values of U and J were calculated for Cr_2O_3, FeO, and Fe_2O_3. Specific results pertaining to each of these systems are discussed in what follows.

1. Cr_2O_3

The values of U and J were calculated for Cr_2O_3 using the method described in Sec. II. As noted above, these parameters were also evaluated using our earlier *ab initio* approach, and thus it will be useful to compare the results obtained through the two methods. The values of U, J, and U-J for a series of AFM Cr_xO_y clusters with the Stuttgart basis set on Cr are shown in Fig. 1. The data demonstrate that all three quantities are converged to within better than 0.2 eV for clusters larger than $Cr_{27}O_{84}^{87-}$. This level of convergence is sufficient for subsequent use in DFT+U calculations, the results of which are relatively insensitive to changes of $\sim \pm 0.5$ eV in U-J. Based on the data, converged values of U, J, and U-J are 3.3, 0.1, and 3.2 eV, respectively.

The calculated value of U-$J = 3.2$ eV is significantly lower than the value of 7.7 eV obtained through our earlier *ab initio* method for evaluating U and J.[20] In our earlier

method, expressions similar to those in Eqs. (11) and (12) were evaluated using the subset of MOs that could be associated with the t_{2g} states of the Cr atom of interest. Meanwhile, the current method employs the full set of MOs. As a result, the new approach encompasses all of the d electrons and associated interactions included in the earlier method, plus interactions between electrons of d-character localized on the Cr atom of interest that are associated with MOs that do not correspond to the t_{2g} states of that atom. Since the on-site Coulomb and exchange interactions included in the previous method correspond to those between the most localized states with the largest d occupations, it is anticipated that the additional on-site interactions captured by considering the full set of MOs will be smaller than those captured in the earlier method. At the same time, considering additional MOs will increase the populations of the d orbitals. Taken together, these two effects cause the denominators in Eqs. (20) and (21) to increase more rapidly than the numerators, leading to smaller values of U and J. Since the expression for U [Eq. (20)] includes interactions between electrons of opposite spin, which would not have been captured for this system with the earlier method and are not included in the definition of J [Eq. (21)], the value of U is more significantly affected than J, leading to a decrease in U-J.

The value of U-J=3.2 eV is similar to the empirically determined value of 4.0 eV, which best reproduces the experimental properties of bulk chromia when used in DFT+U calculations with the LDA, Perdew-Burke-Ernzerhof (PBE), and PW91 functionals.[15,20] This indicates that, at least for this system, the *ab initio* approach reported in Sec. II provides a value of U-J that is in better agreement with the empirical value of this parameter than that obtained with our earlier approach. To the best of our knowledge, values of U and J for chromia have not been calculated previously, aside from our own work mentioned above, and thus there are no calculated values against which we can directly compare our results. However, U and J have been evaluated for Cr ions in perovskites using constrained local density approximation (LDA) calculations.[38] In that study, U was estimated at between 2 and 8 eV, depending on which electrons were treated as localized. Clearly, the value of U obtained in this work falls within this rather wide range of values. The value of J reported in the constrained LDA study was ~1.0 eV and we note that it is standard practice to assume that J =1.0 eV in DFT+U studies. Meanwhile, our calculated value of J is 0.1 eV and we never find J to be as high as 1.0 eV, even for the smallest cluster considered. By contrast, the calculated value of J for an isolated Cr^{3+} ion is 0.9 eV. The difference between the ionic value and that obtained with the largest cluster is significant, and suggests that strong delocalization of the Cr $3d$ orbitals occurs. In general, J should be much smaller than U and should tend toward zero as the cluster increases in size, due to the structure of the integrals involved (orbital products in the numerator of the integrand) in the computation of J. This is precisely why exchange-correlation is short-ranged and why J is always much smaller than U.
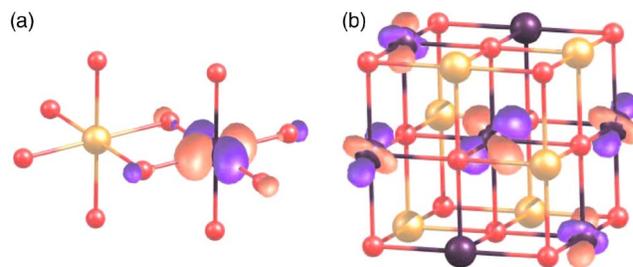

FIG. 2. (Color online) (a) $Fe_2O_{10}^{16-}$ and (b) $Fe_{13}O_{38}^{50-}$ clusters with one canonical UHF MO plotted at an isosurface value of 0.08 a.u. The iron atoms are larger than the oxygen atoms. Iron atoms with opposite spins are represented by different shadings. Solid lines indicate bonds within the cluster. Note that some of the oxygen atoms are not shown for a clearer view of the MOs. In (a), the Fe^{2+} under consideration is on the right. In (b), the Fe^{2+} iron under consideration is the one located at the center of the cube. The different shades of the MOs indicate opposite signs of the wavefunction. The LANL2DZ basis set was used for Fe, and the 6-31G(d) basis set was used for O.

2. FeO

Values of U and J were also calculated for FeO. As noted above, the electronic structure of this system did not permit the unambiguous identification of canonical UHF MOs of a highly localized nature, which was central to our earlier approach for evaluating U and J. This is evident from Fig. 2, which shows one canonical UHF MO for each of the $Fe_2O_{10}^{16-}$ and $Fe_{13}O_{38}^{50-}$ clusters. For the smaller cluster, the MO clearly corresponds to a $3d$ orbital localized on one of the Fe centers; however, the system is too small to yield converged values of U and J. Meanwhile, for the larger cluster, the canonical UHF MO shown is clearly associated with the $3d$ electrons on Fe, but is distributed over many atomic centers and thus not suited to calculating U and J with the earlier method. This delocalization is typical of the electronic structures of the larger Fe_xO_y clusters. Tests demonstrated that calculating U and J with the earlier procedure using localized orbitals, i.e., MOs obtained by localizing the canonical UHF MOs through a unitary transformation of the orbitals, leads to values of U-J that are far too large to be used in DFT+U calculations, which is a consequence of the lack of rotational invariance associated with the earlier method. The method described in Sec. II overcomes the limitations of the earlier method by using the entire set of UHF MOs, which eliminates the need to specify particular orbitals for use in the calculation of U and J and retains rotational invariance.

The calculated values of U, J, and U-J for FeO as a function of system size are shown in Fig. 3 for a series of AFM clusters with the Stuttgart basis set applied to Fe. The results demonstrate that J is converged to within 0.1 eV for the largest cluster, yielding a value of J=0.2 eV for this system. Meanwhile, the values of U and U-J change by 0.4 and 0.3 eV, respectively, upon moving from the second-largest to largest clusters. Additional calculations on a set of FM clusters (see Table I) yielded values of U=3.7 eV and U-J =3.6 eV, which were converged to within 0.1 eV. Due to superexchange effects, in which two magnetic ions have magnetic interactions through their common nonmagnetic neighbors, it is anticipated that the d orbitals of FM systems
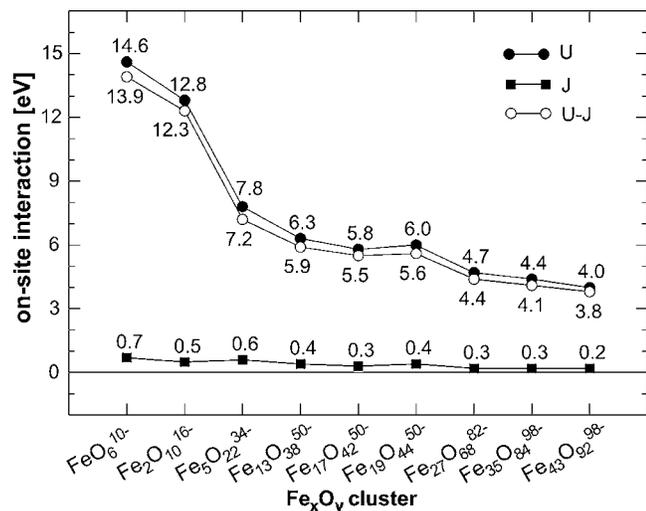
FIG. 3. U, J, and U-J for FeO as a function of cluster size. The clusters exhibited AFM spin ordering. All calculations were performed using the Stuttgart basis set on iron and a 6-31G(d) basis set on oxygen. Based on a comparison with the corresponding ferromagnetic systems, converged values of U, J, and U-J are 3.9, 0.2, and 3.7 eV, respectively.

will be less localized than those in the AFM systems. As a consequence, the values of U and U-J for FM systems should be (and are) lower than those for the corresponding AFM systems. Since, we expect the values for the AFM systems to be higher, we suggest U-J=3.7 eV to be a good estimate of the converged value for the AFM clusters with the Stuttgart basis set on Fe. This value is in excellent agreement with that previously determined empirically for FeO (3.5 eV) (Ref. 39) and is consistent with the low end of values of U-J obtained through constrained DFT+U calculations for Fe in FeO (ranging from 4 to 6 eV).[18,40,41] As mentioned above, it was not possible to obtain a reasonable value of U-J for FeO with our earlier *ab initio* method, whereas the current approach yields a value for this quantity that is suitable for DFT+U calculations. Overall, this illustrates how the new approach improves upon some of the practical limitations of our previous method.

3. Fe$_2$O$_3$

U and J also were calculated for Fe$_2$O$_3$. As noted above, due to a contraction of the 3d states, it is anticipated that the Fe^{3+} ions in this material should have values of U and J that are higher than those of the Fe^{2+} ions in FeO. Thus, by comparing the calculated values of U and J for Fe$_2$O$_3$ with those calculated for FeO we will be able to assess the sensitivity of the methodology to the oxidation state of the transition metal ion. The values of U, J, and U-J as a function of system size are shown in Fig. 4 for a series of AFM clusters with the Stuttgart basis set applied to Fe. The values of U, J, and U-J are converged to better than 0.3 eV for the largest cluster. Since there is a slight variation among the values for the three largest clusters, we have averaged them to obtained converged values of 4.6, 0.3, and 4.3 eV for U, J, and U-J, respectively.

The converged value of U-J=4.3 eV is 1.3 eV higher than the empirical value of 3.0 eV reported by Rollmann *et al.* for use with the PW91 functional (although their results

suggest higher values of U-J also can adequately reproduce experimental data),[42] and the empirical value of 0.95 eV reported by Punkkinen *et al.* for use with LDA.[43] These empirical values are actually lower than the empirical value of 3.5 eV determined previously for FeO,[39] whereas the value of U-J for Fe$_2$O$_3$ should be higher than that for FeO due to the higher oxidation number of iron in the former material. Thus, it seems that the empirical values for Fe$_2$O$_3$ and FeO, while best reproducing experimental results when used in DFT+U calculations may not reflect accurately the underlying physical meanings of the parameters U and J. This highlights the deficiencies of relying on a limited number of experimental data to determine U-J empirically. Meanwhile, the calculated value of U-J=4.3 eV for Fe$_2$O$_3$ is 0.6 eV higher than the calculated value of U-J=3.7 eV for FeO we reported above. Overall, this demonstrates that the method developed in this work is able to distinguish between transition metal ions in different oxidation states, with U-J exhibiting the same dependence on the oxidation number of the transition metal ion that is anticipated on the basis of arguments regarding the contraction of the localized orbitals.

C. Dependence on electronic structure and basis set

Additional calculations were performed on clusters with FM electronic structures and with the LANL2DZ basis set applied to the transition metal atoms. The values of U, J, and U-J obtained through these additional calculations exhibited the same general convergence behavior as the data shown in Figs. 1, 3, and 4. Figures showing these results can be found in the Supplementary Information.[44] The converged values of U, J, and U-J obtained through the whole series of calculations are summarized in Table I.

The data in Table I demonstrate that the values of U, J, and U-J are relatively insensitive to the basis set used on the transition metal atoms, with the largest difference between any values obtained with the LANL2DZ and Stuttgart basis sets being a change of 0.2 eV in the value of U for antiferromagnetic Cr$_2$O$_3$ and FeO. This observation is important because it indicates that the smaller LANL2DZ basis set can be used to evaluate U and J through this procedure, which will decrease the computational expense of the calculations.

The data also reveal that the values of U, J, and U-J for the AFM systems are consistently larger than those for the corresponding FM systems, the sole exception being Cr$_2$O$_3$ with the Stuttgart basis set where J is the same in both cases. As discussed above, superexchange effects will cause the d orbitals of the FM systems to be less localized than those in the AFM systems, leading to lower values of U, J, and U-J in the former. The results indicate that the method captures this trend. In terms of the values themselves, the results indicate that, in some cases, significantly different values of U and U-J are obtained for the FM and AFM systems. For example, the results for Cr$_2$O$_3$ are relatively insensitive to the spin ordering, while the values of U and U-J can change by as much as 0.8 eV for Fe$_2$O$_3$. Since a change of 0.8 eV in the value of U-J is sufficiently large to affect the results of DFT+U calculations, these results suggest that care must be

TABLE I. Values of U, J, and U-J for Cr_2O_3, FeO, and Fe_2O_3 with different basis sets on M (M=Cr or Fe) and different ordering of net spins.

Basis set on M	Spin ordering	U (eV)	J (eV)	U-J (eV)
	Cr_2O_3			
Stuttgart	Antiferromagnetic	3.3	0.1	3.2
Stuttgart	Ferromagnetic	3.3	0.1	3.2
LANL2DZ	Antiferromagnetic	3.5	0.2	3.3
LANL2DZ	Ferromagnetic	3.4	0.1	3.3
	FeO			
Stuttgart	Antiferromagnetic	3.9[a]	0.2	3.7[a]
Stuttgart	Ferromagnetic	3.7	0.1	3.6
LANL2DZ	Antiferromagnetic	4.1	0.2	3.9
LANL2DZ	Ferromagnetic	3.7	0.1	3.6
	Fe_2O_3			
Stuttgart	Antiferromagnetic	4.6	0.3	4.3
Stuttgart	Ferromagnetic	3.9	0.2	3.7
LANL2DZ	Antiferromagnetic	4.7	0.3	4.4
LANL2DZ	Ferromagnetic	3.9	0.2	3.7

[a]Converged values of U and U-J for this particular system were taken to be slightly higher than those for the corresponding ferromagnetic system. The values of U and U-J in the largest cluster for this system were 4.0 and 3.8 eV, respectively.

taken in ensuring that the spin ordering in the clusters used to determine U and J through the ab initio approach accurately reflects that of the bulk material.

IV. BULK CALCULATIONS

The utility of a particular value of U-J is determined ultimately by its ability to reproduce experimental data when used in DFT+U calculations. In order to assess the usefulness of the values of U-J calculated in the preceding section, DFT+U calculations of bulk Cr_2O_3, Fe_2O_3, and FeO were performed using these values. The details of these calculations are provided in Sec. IV A, and the results are discussed in Sec. IV B.

A. Calculation details

DFT+U calculations of bulk Cr_2O_3, Fe_2O_3, and FeO were performed with the VASP simulation package[24,25] using the DFT+U formalism of Dudarev et al.[23] The values of U-J used in these calculations corresponded to those calculated above (3.2 eV for Cr_2O_3, 4.3 eV for Fe_2O_3, and 3.7 eV for FeO). Calculations were performed using the spin-polarized LDA (Ref. 45) and PBE (Ref. 46) generalized gradient approximation (GGA) exchange-correlation functionals. The nuclei and core electrons were described with the projector augmented wave potentials[47,48] provided with VASP, with the $1s$ electrons of oxygen and $1s$, $2s$, $2p$, and $3s$ electrons of transition metal atoms included in the core. The valence electrons were described by a plane-wave basis. The net spins were assigned in a manner consistent with the observed AFM ground state ordering in each of these materials.

The calculations of Cr_2O_3 were performed using a model consisting of the bulk hexagonal unit cell of this material. All calculations of this material employed a 550 eV plane-wave cutoff and a Γ-point centered $3 \times 3 \times 1$ k-point grid, along
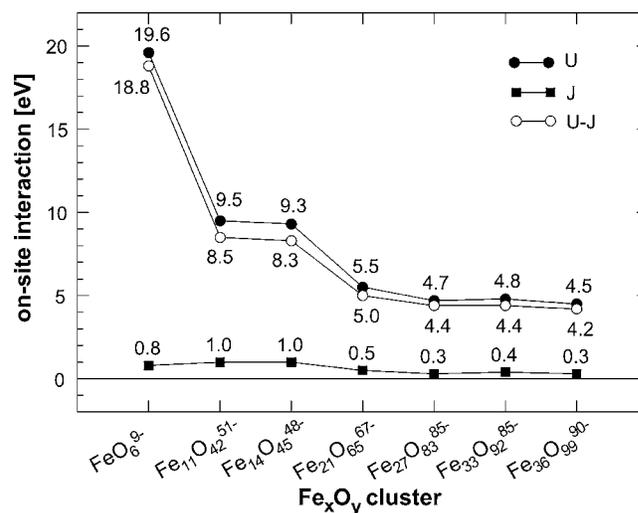

FIG. 4. U, J, and U-J for Fe_2O_3 as a function of cluster size. The clusters exhibited AFM spin ordering. All calculations were performed using the Stuttgart basis set on iron and a 6-31G(d) basis set on oxygen. Converged values of U, J, and U-J are 4.6, 0.3, and 4.3 eV, respectively.

with Gaussian smearing with a smearing width of 0.1 eV. The only exception to this approach was in the evaluation of the band gap, where a $9 \times 9 \times 3$ k-point grid in conjunction with the tetrahedron method[49,50] with corrections by Blöchl et al.[51] was used for increased sampling of the Brillouin zone. 26 additional empty bands were included in all calculations of Cr_2O_3.

The calculations of Fe_2O_3 were performed using a single rhombohedral primitive unit cell of this material. The plane-wave cutoff for this system was 700 eV and a Monkhorst-Pack $4 \times 4 \times 4$ k-point grid was used, along with Gaussian smearing with a smearing width of 0.01 eV. The only exception to this approach was the evaluation of the band gap, which employed a Monkhorst–Pack $12 \times 12 \times 12$ k-point grid with the tetrahedron method with the corrections of Blöchl et al. All calculations of Fe_2O_3 employed 10 additional empty bands.

FeO calculations were performed using a single rhombohedral unit cell containing two formula units. A plane-wave cutoff of 700 eV and a Monkhorst–Pack $8 \times 8 \times 8$ k-point grid was used. Gaussian smearing with a smearing width of 0.2 eV was necessary to obtain smooth equation of state curves in PBE+U calculations. Furthermore, in order to obtain a nonmetallic ground state of FeO at the PBE+U level of theory, it was necessary to allow the system to break rhombohedral symmetry. Smearing was not necessary and therefore not used in the LDA+U calculations of this material. At the LDA+U level, the band gaps calculated with and without enforcing symmetry differed by 0.2 eV. We report only the LDA+U results for FeO in which symmetry was not enforced. For the calculation of the band gap in FeO, integration over the Brillouin zone was performed using a $16 \times 16 \times 16$ k-point grid with the tetrahedron method including corrections of Blöchl et al.

For all materials considered, these numerical parameter sets converged the total energies to better than 1 meV/atom

TABLE II. Experimental and calculated properties of bulk Cr_2O_3, Fe_2O_3, and FeO. Calculations were performed using the converged *ab initio* values of *U-J*.

Property	LDA+U	PBE+U	Expt.[a]
	Cr_2O_3		
V^b (Å^3)	285.03	306.22	287.98
$|\mathbf{a}|^c$ (Å)	4.930	5.052	4.961
$|\mathbf{c}|^c$ (Å)	13.541	13.853	13.599
B^d (GPa)	238.8	198.6	238.4
E_{gap}^e (eV)	2.8	2.9	3.4
μ^f (μ_B)	2.8	2.9	3.8
	$Fe_2O_3^g$		
V^b (Å^3)	96.95	104.38	100.60
$|\mathbf{a}|^c$ (Å)	4.972	5.098	5.035
$|\mathbf{c}|^c$ (Å)	13.587	13.915	13.747
B^d (GPa)	223.4	190.2	178, 225
E_{gap}^e (eV)	1.9	2.1	1.9
μ^f (μ_B)	4.1	4.2	4.6–4.9
	FeO^h		
V^b (Å^3)	38.00	42.47	40.70
$|\mathbf{a}|^c$ (Å)	5.251	5.449	5.308
$|\mathbf{b}|^c$ (Å)	5.247	5.308	5.308
$|\mathbf{c}|^c$ (Å)	5.333	5.318	5.308
α^i (deg)	32.2	33.9	33.6
β^i (deg)	32.3	33.8	33.6
γ^j (deg)	33.5	33.9	33.6
B^d (GPa)	211	157	142, 180
E_{gap}^e (eV)	1.6	1.1	2.4
μ^f (μ_B)	3.6	3.6	4.2

[a]Experimental data for Cr_2O_3 are from Refs. 33–35 and 54–56, for Fe_2O_3 are from Refs. 55, 57, and 58, and for FeO are from Refs. 59–63.
[b]Volume.
[c]Lengths of lattice vectors **a**, **b**, and **c**.
[d]Bulk modulus.
[e]Band gap.
[f]Magnetic moment.
[g]The calculated data for Fe_2O_3 were converted from the rhombohedral to hexagonal representations to facilitate comparison against experiment.
[h]The experimental data for FeO were converted from the cubic to rhomohedral representations to facilitate comparison.
[i]Cell angles of the rhombohedral unit cell.

and the elements of the stress tensor to better than 2 kbar with respect to results obtained with higher plane-wave cutoffs and denser *k*-point grids.

The cell and ionic positions were fully relaxed for each material and exchange-correlation functional. The energy versus volume curves used to calculate the bulk moduli were obtained by uniformly expanding the unit cell for a series of volumes around the optimized structures and relaxing the ionic positions at each volume, subject to the constraint that the cell volume and shape remain unchanged. The bulk moduli were determined by fitting the resulting energy versus volume data to a third-order Birch–Murnaghan equation of state.[52,53]

B. Results

The results of the DFT+U calculations of Cr_2O_3, Fe_2O_3, and FeO are summarized in Table II and are discussed below.

1. Cr_2O_3

The structural data and bulk modulus obtained through the LDA+U calculations of Cr_2O_3 are in good agreement with experimental data:[55,56] Calculated and experimental values agree to within 1%. The band gap at the LDA+U level is "underestimated" by 0.6 eV;[33–35] however, we note that the calculated value is based on a difference in the eigenvalues of Kohn–Sham orbitals and does not account for final state relaxation effects present in the measurements (the experimental value is based on photoemission/inverse photoemission experiments). As such, the calculated and experimental values should not agree anyway. The LDA+U value of the magnetic moment is significantly too low;[54] however, this large discrepancy may be due to the fact that the experimental value was based on a purely ionic model of Cr_2O_3, whereas it is known that significant interaction between the O 2*p* states and Cr 3*d* states exists in this material. Consideration of such interactions would reduce the residual magnetic moment, thereby bringing the experimental values into better agreement with the calculated values. The data obtained with the PBE functional are less promising. The calculated band gap and magnetic obtained with PBE are a slight improvement over the values obtained with LDA, but still differ significantly from the experimental values. The structural data and bulk modulus obtained in the PBE+U calculations are in much worse agreement with experiment than the results of the LDA+U calculations. Overall, the results indicate that using the LDA functional in conjunction with a value of *U-J*=3.2 eV yields results that are in good agreement with experiment, while the results obtained with the PBE functional are less accurate upon comparison with experimental values. This should not be taken as a deficiency of the calculated value of *U-J*, however, as previous studies have demonstrated that no single value of *U-J* used in conjunction with the PBE functional is able to reproduce accurately both the structural and electronic properties of Cr_2O_3. As such, the poor results obtained with PBE seem to be a deficiency of using this functional to study Cr_2O_3 in DFT+U calculations instead of a failure of our calculated value of *U-J*. The reader interested in more detailed investigations of how the calculated properties of bulk Cr_2O_3 vary with value of *U-J* is directed for Ref. 20 for work using the LDA and PBE functionals and Ref. 15 for work performed with the PW91 functional.

2. Fe_2O_3

In the case of Fe_2O_3, both the LDA+U and PBE+U calculations performed with the calculated value of *U-J*=4.3 eV yield results that are in good agreement with the experimental data.[55,57,58] Note that the calculated structural data were converted from the rhombohedral representation to a hexagonal representation to facilitate a comparison with experimental data. The LDA+U volume and lattice constants are slightly lower than the experimental values, while the PBE+U quantities are slightly higher. In the case of the lattice constants, both methods yield values that are within $\sim \pm 1\%$ of experiment. Meanwhile, the calculated volumes both agree with experiment to within approximately 3.5%,

with the volume underestimated by LDA+U and overestimated by PBE+U. The PBE+U value of the bulk modulus is lower than that obtained with LDA+U, but due to discrepancies in the experimental values it is not possible to state which value is in better agreement with experiment. Both methods reproduce the experimental optical band gap to within 0.1 eV;[57] however, once again we note that the calculated band gap does not correspond to the same quantity measured in experiments, so the agreement should be considered fortuitous. Both methods underestimate the magnetic moment by approximately the same amount. Overall, these results indicate that the value of U-J=4.3 eV used in conjunction with either the LDA or PBE functionals is able to reproduce fairly well the measured properties of Fe_2O_3. The reader interested in a more detailed analysis of how the properties of bulk Fe_2O_3 vary with the value of U-J is directed to Ref. 42.

3. FeO

The results of the LDA+U and PBE+U calculations of FeO obtained with U-J=3.7 eV are summarized in Table II. The experimental values[59,60,63] reported in that table have been converted from the cubic lattice for comparison against the calculated values, which were obtained using a rhombohedral unit cell. The data show that LDA+U underestimates the volume by ~7%, while PBE+U overestimates this quantity by ~4%. The optimized lattice vectors of the simulation cell are inequivalent in both the LDA+U and PBE+U calculations, indicating that the material prefers to break rhombohedral symmetry. On average, the lattice constants calculated at the LDA+U level are ~0.6% smaller than the experimental values, whereas the PBE+U calculations overestimate the lattice constants by ~1%. The LDA+U calculations underestimate the cell angle, which corresponds to an elongation of the unit cell along the [111] direction. Such elongation is consistent with experimental observations,[59,60] with an angle of 33.2° being measured for the distorted structure. (The value of the cell angle in Table II corresponds to a nondistorted cubic structure, and so is slightly different from 33.2°.) Meanwhile, the PBE+U calculations yield a large cell angle, indicative of a compression along the [111] direction. This incorrect prediction by PBE+U has been observed and discussed previously by Cococcioni and de Gironcoli.[18] The LDA+U value of bulk modulus is higher than experimental values, due to the typical overbinding by the LDA, while the PBE+U result is within the range of available experimental values. Both methods underestimate the experimental optical band gap of 2.4 eV;[61] however, once again, we point out that the calculated band gap does not correspond to the actual quantity being measured (in this case, the measurement is of an excitation energy). Both methods underestimate the magnetic moment[62] by 0.6 μ_B. The discrepancies between the experimental and calculated values have been attributed to an orbital magnetic moment contribution that could be as large as 1 μ_B, which is not accounted for in the DFT+U theory. When such spin-orbit effects are included, this brings DFT+U results in better agreement with

experiment.[10] As a whole, the results indicate that LDA+U calculations provide a better representation of the bulk properties of FeO than do PBE+U calculations.

V. CONCLUSIONS

We have reported a new *ab initio* method for evaluating the parameters U and J that enter into the DFT+U energy functional. This method is based on a relationship between these parameters and the Coulomb and exchange integrals evaluated using the entire set of unrestricted Hartree-Fock (UHF) molecular orbitals (MOs) for an electrostatically embedded cluster representing the bulk material of interest. The use of the entire set of UHF MOs eliminates the need to determine which MOs correspond to localized states and renders the method invariant to unitary transformations of the entire set of UHF MOs. These features overcome two significant limitations of a similar *ab initio* approach we developed previously. The values of U-J obtained through this approach also have the advantage of being derived from a method that is free of self-interaction errors, unlike constrained DFT calculations. Moreover, the *ab initio* approach does not rely on experimental data, thereby enabling the use of DFT+U calculations in a fully predictive sense.

The new *ab initio* method was used to evaluate U and J for Cr_2O_3, Fe_2O_3, and FeO. The converged values of U-J for each of these materials (3.2 eV for Cr_2O_3, 4.3 eV for Fe_2O_3, and 3.7 eV for FeO) are in good agreement with empirical estimates of these parameters, thereby validating our new scheme. The calculated values of U and J also exhibit the anticipated dependence upon the ionic charge and ordering of net spins in the material. In particular, the calculated value of U-J for FeO is lower than that of Fe_2O_3, which is consistent with the higher ionic charge of the iron ions in Fe_2O_3, leading to a more pronounced contraction of the 3d orbitals and hence a larger value of U-J for Fe_2O_3. It was also found that the calculated values of U-J for each of these materials obtained with antiferromagnetic spin orderings were slightly higher than those obtained with ferromagnetic spin orderings. This is anticipated because superexchange effects will cause the 3d orbitals in ferromagnetic systems to be less localized than those in antiferromagnetic systems, leading to lower values of U-J for the former.

DFT+U calculations were performed using the calculated values of U-J in conjunction with the LDA and PBE functionals. In general, the results obtained in these calculations were in good agreement with experimental data; in most cases, the results obtained through the LDA+U calculations were in better agreement with experiment than those obtained with PBE+U. Overall, these results indicate that the *ab initio* method for calculating U and J is suitable for performing accurate and fully predictive DFT+U calculations of strongly correlated electron materials.

[1] N. I. Gidopoulos, in *Handbook of Molecular Physics and Quantum Chemistry* (Wiley, West Sussex, 2003), Vol. 2, p. 52.

[2] J. Kohanoff and N. I. Gidopoulos, in *Handbook of Molecular Physics and Quantum Chemistry* (Wiley, West Sussex, 2003), Vol. 2, p. 532.

[3] F. M. Bickelhaupt and E. J. Baerends, in *Reviews in Computational Chemistry* (Wiley-VCH, New York, 2000), Vol. 15, p. 1.

[4] W. Kohn and L. J. Sham, Phys. Rev. **140**, A1133 (1965).

[5] P. Hohenberg and W. Kohn, Phys. Rev. **136**, B864 (1964).

[6] C. Pisani, M. Busso, G. Capecchi, S. Casassa, R. Dovesi, L. Maschio, C. Zicovich-Wilson, and M. Schutz, J. Chem. Phys. **122**, 094113 (2005).

[7] V. Bezugly and U. Birkenheuer, Chem. Phys. Lett. **399**, 57 (2004).

[8] P. Y. Ayala, K. N. Kudin, and G. E. Scuseria, J. Chem. Phys. **115**, 9698 (2001).

[9] J. Q. Sun and R. J. Bartlett, J. Chem. Phys. **104**, 8553 (1996).

[10] F. Tran, P. Blaha, K. Schwarz, and P. Novak, Phys. Rev. B **74**, 155108 (2006).

[11] P. Novak, J. Kunes, L. Chaput, and W. E. Pickett, Phys. Status Solidi B **243**, 563 (2006).

[12] I. de P.R. Moreira, F. Illas, and R. L. Martin, Phys. Rev. B **65**, 155102 (2002).

[13] V. I. Anisimov, F. Aryasetiawan, and A. I. Liechtenstein, J. Phys.: Condens. Matter **9**, 767 (1997).

[14] S. L. Dudarev, A. I. Liechtenstein, M. R. Castell, G. A. D. Briggs, and A. P. Sutton, Phys. Rev. B **56**, 4900 (1997).

[15] A. Rohrbach, J. Hafner, and G. Kresse, Phys. Rev. B **70**, 125426 (2004).

[16] O. Bengone, M. Alouani, P. Blöchl, and J. Hugel, Phys. Rev. B **62**, 16392 (2000).

[17] V. I. Anisimov and O. Gunnarsson, Phys. Rev. B **43**, 7570 (1991).

[18] M. Cococcioni and S. de Gironcoli, Phys. Rev. B **71**, 035105 (2005).

[19] H. J. Kulik, M. Cococcioni, D. A. Scherlis, and N. Marzari, Phys. Rev. Lett. **97**, 103001 (2006).

[20] N. J. Mosey and E. A. Carter, Phys. Rev. B **76**, 155123 (2007).

[21] M. S. Gordon and M. W. Schmidt, in *Theory and Applications of Compuational Chemistry, the First Forty Years*, edited by C. E. Dykstra, G. Frenking, K. S. Kim, and G. E. Scuseria (Elsevier, Amsterdam, 2005).

[22] M. W. Schmidt, K. K. Baldridge, J. A. Boatz, S. T. Elbert, M. S. Gordon, J. H. Jensen, S. Koseki, N. Matsunaga, K. A. Nguyen, S. J. Su, T. L. Windus, M. Dupuis, and J. A. Montgomery, J. Comput. Chem. **14**, 1347 (1993).

[23] S. L. Dudarev, G. A. Botton, S. Y. Savrasov, C. J. Humphreys, and A. P. Sutton, Phys. Rev. B **57**, 1505 (1998).

[24] G. Kresse and J. Furthmüller, Comput. Mater. Sci. **6**, 15 (1996).

[25] G. Kresse and J. Hafner, Phys. Rev. B **47**, 558 (1993).

[26] P. J. Hay and W. R. Wadt, J. Chem. Phys. **82**, 284 (1985).

[27] R. D. Shannon, Acta Crystallogr., Sect. A: Cryst. Phys., Diffr., Theor. Gen. Crystallogr. **32**, 751 (1976).

[28] H. M. Evjen, Phys. Rev. **39**, 675 (1932).

[29] T. H. Dunning, Jr., J. Chem. Phys. **90**, 1007 (1989).

[30] W. J. Hehre, R. Ditchfield, and J. A. Pople, J. Chem. Phys. **62**, 2921 (1975).

[31] T. J. Dunning, Jr., J. Chem. Phys. **53**, 2823 (1970).

[32] M. Dolg, U. Wedig, H. Stoll, and H. Preuss, J. Chem. Phys. **86**, 866 (1987).

[33] T. G. Worlton, R. M. Brugger, and R. B. Bennion, J. Phys. Chem. Solids **29**, 435 (1968).

[34] T. R. McGuire, E. J. Scott, and F. H. Grannis, Phys. Rev. **102**, 1000 (1956).

[35] B. N. Brockhouse, J. Chem. Phys. **21**, 961 (1953).

[36] J. B. Goodenough, Prog. Solid State Chem. **5**, 145 (1971).

[37] C. G. Shull, W. A. Strauser, and E. O. Wollan, Phys. Rev. **83**, 333 (1951).

[38] I. Solovyev, N. Hamada, and K. Terakura, Phys. Rev. B **53**, 7158 (1996).

[39] J. Zaanen and G. A. Sawatzky, J. Solid State Chem. **88**, 8 (1990).

[40] W. E. Pickett, S. C. Erwin, and E. C. Ethridge, Phys. Rev. B **58**, 1201 (1998).

[41] V. I. Anisimov, J. Zaanen, and O. K. Andersen, Phys. Rev. B **44**, 943 (1991).

[42] G. Rollman, A. Rohrbach, P. Entel, and J. Hafner, Phys. Rev. B **69**, 165107 (2004).

[43] M. P. J. Punkkinen, K. Kokko, W. Hergert, and I. J. Vayrynen, J. Phys.: Condens. Matter **11**, 2341 (1999).

[44] See EPAPS Document No. E-JCPSA6-129-623825 for detailed information regarding the models used to evaluate U and J, and for additional plots demonstrating the convergence of U and J for Cr_2O_3, FeO, and Fe_2O_3 clusters in different magnetic states and/or with different basis sets than those used in the main text. For more information on EPAPS, see http://www.aip.org/pubservs/epaps.html.

[45] J. P. Perdew and A. Zunger, Phys. Rev. B **23**, 5048 (1981).

[46] J. P. Perdew, K. Burke, and M. Ernzerhof, Phys. Rev. Lett. **77**, 3865 (1996).

[47] G. Kresse and D. Joubert, Phys. Rev. B **59**, 1758 (1999).

[48] P. Blöchl, Phys. Rev. B **50**, 17953 (1994).

[49] O. Jepsen and O. K. Andersen, Solid State Commun. **9**, 1763 (1971).

[50] G. Lehmann and M. Taut, Phys. Status Solidi B **54**, 469 (1972).

[51] P. Blöchl, O. Jepsen, and O. K. Andersen, Phys. Rev. B **49**, 16223 (1994).

[52] F. Birch, Phys. Rev. **71**, 809 (1947).

[53] F. D. Murnaghan, Proc. Natl. Acad. Sci. U.S.A. **30**, 2344 (1944).

[54] R. Zimmermann, P. Steiner, and S. Hüfner, J. Electron Spectrosc. Relat. Phenom. **78**, 49 (1996).

[55] L. W. Finger and R. M. Hazen, J. Appl. Phys. **51**, 5362 (1980).

[56] R. E. Newnham and Y. M. de Haan, Z. Kristallogr. **117**, 235 (1962).

[57] F. J. Morin, Phys. Rev. **93**, 1195 (1954).

[58] Y. Sato and S.-i. Akimoto, J. Appl. Phys. **50**, 5285 (1979).

[59] N. C. Tombs and H. P. Rooksby, Nature (London) **165**, 442 (1950).

[60] B. T. M. Willis and H. P. Rooksby, Acta Crystallogr. **6**, 827 (1953).

[61] I. Balberg and H. L. Pinch, J. Magn. Magn. Mater. **7**, 12 (1978).

[62] P. D. Battle and A. K. Cheetham, J. Phys. C **12**, 337 (1979).

[63] C. A. McCammon and L.-g. Liu, Phys. Chem. Miner. **10**, 106 (1984).